Journal of the European Ceramic Society 22 (2002) 2187–2196

www.elsevier.com/locate/jeurceramsoc

Thermal shock and thermal fatigue study of alumina

P.K. Panda[a,*], T.S. Kannan[a], J. Dubois[b], C. Olagnon[b], G. Fantozzi[b]

[a]*Materials Science Division, National Aerospace Laboratories, Bangalore-17, India*
[b]*GEMPPM, INSA de Lyon, 69621,Villeurbanne Cedex, France*

Received 11 May 2000; received in revised form 28 December 2001; accepted 12 January 2002

Abstract

Preliminary results on the thermal shock and thermal fatigue behaviour of alumina studied in a newly designed novel and simple test equipment are reported. The top surface of a test sample was heated by an oxy-hydrogen flame while the opposite surface was cooled to generate temperature and thermal stress gradients. The maximum stressed zone and the effect of the thickness of the sample on critical temperature difference (ΔT_C) were studied by conducting actual experiments on plain and indented alumina specimens and also by modelling temperature and thermal stress distribution in the sample using a finite element (FE) software. It was observed that the maximum stress was experienced near the periphery of the top surface and ΔT_C was more for thicker samples. Thermal fatigue study was conducted by varying temperature difference of the fatigue cycles and also by inducing different crack lengths in the sample. It was observed that the fatigue life sharply decreased with increase in initial crack length or by increasing the temperature difference of the fatigue cycles. The acoustic emission (AE) signals corresponding to formation and growth of large number of micro-cracks were observed.

Keywords: Acoustic Emission; Al_2O_3; Finite Element Modeling (FEM); Thermal fatigue; Thermal shock resistance

1. Introduction

There is a growing demand of ceramic materials for high temperature structural applications mainly due to their high melting point and good mechanical strength at high temperature. However, their application is limited due to catastrophic failure of these materials when subjected to sudden change of temperature (thermal shock) or repetitive cycling of temperatures (thermal fatigue). In a thermal shock experiment, when the change in temperature exceeds critical temperature difference (ΔT_C) of the material, the tensile stress generated in the material due to temperature gradient exceeds its actual tensile strength resulting in failure of the material. In thermal fatigue experiments, the material is subjected to repetitive cyclic temperature changes so that a micro-crack with initial crack size a_0 ($a_0 < a_c$) grows incrementally in each cycle till it reaches the critical crack size (a_c) at which the sample fails catastrophically. There are many test methods available to characterise thermal shock[1–5] and thermal fatigue[6] of ceramic materials. They are mostly quench experiments which are descending in nature. However, ceramic materials used in aerospace, heat engines etc. often experience rapid increase in temperature that might result in an ascending thermal shock. To test thermal shock and thermal fatigue in ascending mode of heating, suitable test equipment was fabricated.[7] By using the above equipment, thermal shock and thermal fatigue behaviour of alumina was studied. Many authors had extensively studied thermal shock of alumina by taking various parameters, e.g. temperature,[8] thermal stress distribution[9] and effect of critical grain size[10] on thermal shock.

In this paper, the results of thermal shock and thermal fatigue studies conducted on alumina are presented. The effect of sample thickness on ΔT_C, the effect of initial crack length, the effect of maximum temperature and the effect of the maximum stressed region (crack initiation zone) on thermal shock and thermal fatigue was discussed. The tests were simulated using a finite element (FE) software to obtain the temperature and thermal stress distributions experienced by the specimens and the results were compared with the experimental results.

2. Description of the test equipment

The test equipment is designed to heat one surface of the sample while cooling the opposite surface so as to

* Corresponding author.
E-mail address: pkpanda@css.cmmacs.ernet.in (P.K. Panda).

0955-2219/02/$ - see front matter
PII: S0955-2219(02)00022-5

create temperature as well as thermal stress gradient in side sample as per the equation given below.

$$\sigma = \frac{E\alpha\Delta T}{1-\nu}$$

where, σ = thermal stress, α = coefficient of thermal expansion, ΔT = temperature gradient, ν = Poisson's ratio.

The temperature difference which causes the failure of the material is known as critical temperature difference, ΔT_C, and is generally the temperature difference between the uniformly heated hot body and the quenching medium. In our experiment, the temperature of the sample is not uniform due to localised heating by an oxy-hydrogen flame. Threfore, the "maximum hot temperature" is the characteristic temperature for this type of thermal shock experiments and it could be termed as "failure temperature", T_f, if the sample fails similar to ΔT_C in case of quench experiments.

The sample would fail when thermal stress exceeds the tensile strength of the test material. The sample was heated by an oxy-hydrogen flame over a localized area of 4–5 mm diameter to a temperature till it fails. This localized area can be varied by choosing nozzles with different diameters and by varying the distance of the nozzle from the heating surface. The area was measured easily in case of non-oxide samples such as SiC, Si_3N_4, etc., in which the color of the hot zone was changed after the heating. The thermal fatigue tests were conducted by cycling the heating and cooling cycles with a maximum temperature well below the critical temperature so that the sample fails after number of fatigue cycles.

The cooling plays an important role in temperature distribution, hence, thermal stress distribution in the sample, specifically in transient state, i.e. at the beginning of the thermal shock test. If one surface of the sample is not cooled, the heat loss is prevented and the temperature variation across the thickness as well as in radial direction decreases, therefore, the sample would experience less thermal stress, which could be insufficient to cause the failure of the sample. Therefore, efficient cooling is needed to generate large temperature as well as thermal stress gradient so that the failure of the sample could be achieved.

The efficient cooling was effected by keeping the test sample in contact with a water cooled copper block. The sample was fixed to the copper block by using Al based conducting paste. The thermal mass of copper block is very high compared to the sample and copper being a good conductor, the bottom surface of the sample remains at or very close to room temperature during the thermal shock test. In addition, the water flow rate can be adjusted to effect high rate of heating specifically when the sample requires high failure temperature.

Therefore, the test equipment consists of a sample holder, an oxy-hydrogen flame based heat generation system, a temperature measurement system consisting of an IR pyrometer and a thermocouple and a crack detection system monitored by acoustic emission technique. The sample holder is a cylindrical copper block of 85 mm diameter and 80 mm length with an internal cutout to facilitate water circulation very close to the top surface on which the test sample is placed. The oxy-hydrogen flame is used to heat the sample at the centre and the central hot temperature was measured by a mono-colour IR pyrometer (Model-IRCON Modline plus, series 7000, special 200/2000 °C from M/s IRCON Inc., USA). The temperature at the periphery of the sample was measured by a fast response K-type thermocouple. The tip of the thermocouple is placed perpendicularly to the periphery of the sample with the help of spring loading. The failure of the sample was detected by the acoustic emission set up (M/s. Euro Physical Acoustic Society, France) which picks up the signals/events during failure of the specimen. The set up is comprised of a PZT-5 (R-30) sensor, a cylindrical wave-guide (Haynes alloy based), a filter and an amplifier unit. The wave-guide is placed on top of the sample without touching the copper block and a small cut out on the wave-guide exposes the sample to the oxy-hydrogen flame. The AE data as well as two sets of temperatures were acquired, displayed graphically and stored in a PC. By the use of the microprocessor based programmer-controller, the experiments can be performed under different conditions, e.g. with different oxy-hydrogen flow rates, heat-on and cool-down times and number of cycles of the experiments for fatigue experiments, safety factors such as gas cut-off during experimental failures, ignition of flame by high frequency sparking etc., are the additional features incorporated into the test unit.

The equipment is useful to carry out thermal shock test of materials up to a maximum hot zone temperature of 2000 °C in ascending mode. It is provided with a facility to carry out thermal fatigue tests in automatic mode between the hot and cold temperatures at predetermined heating and cooling rates. Further details of the test equipment are presented in the PhD thesis of one of the authors[7] and have also been communicated for publication.[11] A close view of the sample and the test set up with oxy-hydrogen flame heating during the thermal shock test is presented in Fig. 1.

2.1. Experimental procedures

Circular alumina (99.7% purity) samples of diameter 30 ± 0.1 mm and thickness varying between 2 and 6 mm were used for the tests. One side of the test samples were grounded and polished using diamond suspensions ranging from 16 to 1 μm sequentially and finally polished

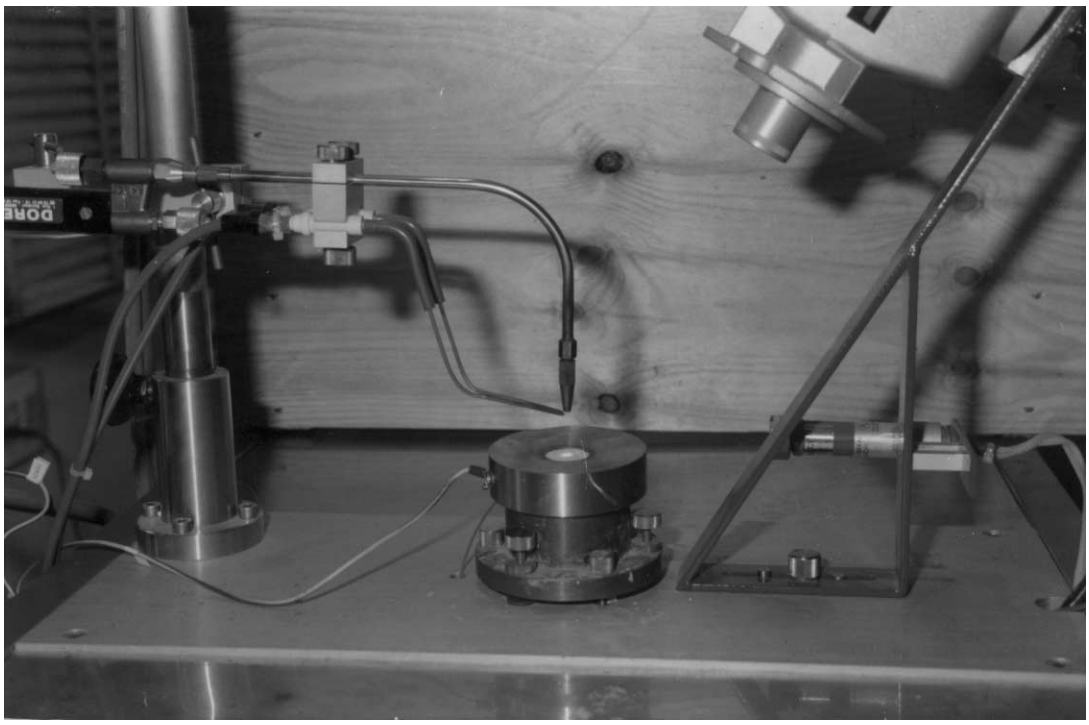

Fig. 1. A close view of the sample and the test set up with oxy-hydrogen flame heating during thermal shock test.

with an alumina suspension of 0.3 μm grain size. The polished samples were annealed at 600 °C for 4 h to relieve the residual stress. The polished surface of the sample was exposed to the flame heating so that the cracks usually generated on top surface of the sample (as explained in the next section) could be detected clearly.

The tests were carried out by placing a test sample on the centre of the copper block by using a conducting paste (Al metal based) in the interface so that the heat could flow efficiently to copper block while providing good contact to the copper block.. The emissivity value of alumina, 0.65, was fixed in the IR panel for accurate measurement of the temperature. This emissivity value was obtained earlier by heating a test sample to a constant temperature that was measured by a thermocouple and also by a pyrometer such that the emissivity value in the pyrometer panel was changed till the temperature measured by the pyrometer was equal to that of the thermocouple. This emissivity value of the pyrometer corresponding to which the temperature reading of the pyrometer as well as thermocouple were equal was 0.65 and this value was taken as the emissivity value of the alumina sample. The tests were repeated in the temperature range of 300–650 °C and the value was found to be constant i.e. 0.65. The oxy-hydrogen gas burner nozzle 100 (corresponding to a gas flow of 100 l/h at NTP) was used for generating the flame. The distance between the nozzle tip and the sample was fixed at 12 ± 0.1 mm. The tests were conducted by selecting suitable oxy-hydrogen gas ratio, the nozzle diameter, the distance of the nozzle from the sample, etc. The oxy-hydrogen flame was ignited automatically by a high voltage spark struck between two metal wires kept close to nozzle.

The tests were also conducted with pre-cracked specimens with known initial crack lengths. These artificial cracks were created using a Vicker's diamond indenture (HSV-20, M/s. Shimadzu, Japan) and the crack lengths were varied by using different loads ranging between 5 and 20 kg. The specimens were subsequently heat treated at 600 °C for 4 h to relieve the residual stress generated while polishing and indentation.

3. Results and discussion

Thermal shock and thermal fatigue studies were carried out on alumina specimens. The experiments were designed to study the total potential of the equipment as well as its limitations. The use of acoustic emission to detect the cracks during the tests was very useful. Two types of acoustic emissions were observed corresponding to the (i) total failure of the material in which either one or a few number of cracks with high intensity were produced and (ii) a large number of acoustic emissions resulted prior to total failure of the sample. These multiple emissions are due to micro-cracking in the sample without causing total failure. The studies on thermal shock tests were first presented followed by those on thermal fatigue.

3.1. Thermal shock tests on alumina specimens

3.1.1. Effect of thickness of the alumina sample on ΔT_C during thermal shock tests

To find the effect of sample thickness on critical temperature difference (ΔT_C) during thermal shock tests, alumina samples of the thickness varying between 2 and 6 mm were subjected to thermal shock tests. The critical temperature difference, ΔT_C, was obtained in each case by substracting the initial temperature of the sample, i.e. the room temperature, 25 °C, from the failure temperature, T_f, at which the sample totally failed. The test results are summarised in the Table 1.

From the results in Table 1, it could be observed that ΔT_C increases with increase in sample thickness.

3.1.2. Effect of indented cracks on ΔT_C

Alumina samples of 3 mm thickness polished to 1 μm finish were indented near the periphery. The indentations were made by applying 5, 10 and 20 kg loads using a Vicker's indentation. Three samples were used for each load. The average crack lengths were measured. The indented samples were subjected to thermal shock tests after annealing at 600 °C for 4 h to find their ΔT_C. The results are summarised in Table 2 and a graph of ΔT_C vs. average crack length is presented in Fig. 2.

3.1.3. Modelling of the test results

To analyse the effect of thickness of the sample on thermal stress, a finite element (FE) software (NISA7.0, M/s. Engineering Mechanics Research Corporation, Bangalore, India) was used for simulation/modelling of the temperature and thermal stress distributions experienced by the samples during the tests. An axis symmetric plane of the sample was created in the form of finite element mesh to which thermo-mechanical properties of the sample were applied. The measured temperature distribution of the hot spot, temperatures at periphery and the temperature of the bottom surface (equal to the out going water temperature due to efficient cooling) were provided as thermal boundary conditions. The temperature values at different distances along the radial direction at the failure were used for modelling. These temperature values were obtained by extrapolation method corresponding to the failure temperature at the centre. The extrapolation was done on the basis of proportional increase in temperature at different radial distances. The details of the procedure followed are given below.

A test sample was heated at the centre up to a temperature well below its critical temperature. The temperatures up to a radial distance of 5 mm from the centre were measured in steps of 1 mm by an IR pyrometer by moving the pyrometer laterally 1 mm each time. It could be noted here that the temperature was very low beyond 5 mm, which could not be measured by IR pyrometer. The temperature values up to 5 mm along with periphery temperature were sufficient for temperature modelling.

The experimental conditions were kept constant so that the temperature at the centre remains the same in each such heating. The temperature distribution at different radial distances thus obtained resulted in one trial. The same was repeated by heating the centre to a higher temperature by changing oxy-hydrogen ratio suitably so that the temperature was still below the failure temperature. The temperature measurements were carried out as explained above to obtain the temperature distribution as trial 2. The oxy-hydrogen ratio was again changed suitably such that the temperature was

Table 1
Failure temperature and ΔT_C of alumina of different thickness

Thickness of the alumina sample (mm)	Failure temperature (°C)	ΔT_C (°C)
2	342±33	317±33
3	390±39	365±39
4	557±75	532±75
5	647±100	622±100
6	700±60	675±60

Table 2
ΔT_C obtained for samples with different indented crack lengths

No.	Load (kg)	Average crack length (μm)	Failure temperature (°C)	ΔT_C (°C)
1	20	481	342	317
2	20	555	405	380
3	20	546	367	342
4	10	343	348	323
5	10	395	268	343
6	5	178	412	387
7	5	149	381	356

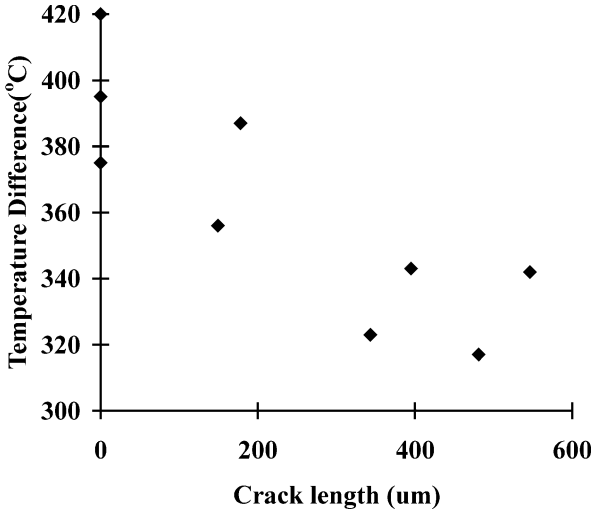

Fig. 2. Critical temperature difference vs. crack length.

increased above the critical temperature and the sample was failed. From the failure temperature and the temperature distributions obtained in last two trials, the temperatures at other radial distances were obtained by extrapolation[7] by using the equation given below:

$$\frac{T3(0) - T2(0)}{T2(0 - T1(0))} = \frac{T3(1) - T2(1)}{T2(1) - T1(1)}$$

where,

$T3(0)$ = The temperature at the centre of the sample measured by the pyrometer at the time of cracking due to thermal shock in trial no. 3.

$T2(0)$ and $T1(0)$ are the temperatures at the centre of the sample measured by the pyrometer in Trial 2 and Trial 1, respectively,

$T2(1)$ and $T1(1)$ are the temperatures at 1 mm radial distance from the centre of the sample measured by pyrometer in Trial 2 and Trial 1, respectively. $T3(1)$ is the extrapolated temperature at 1 mm away from the centre.

The results are presented graphically in Fig. 3. From the failure temperatures of alumina of different thickness, the temperature values at different radial distances were extrapolated and presented graphically in Fig. 4.

By applying the above extrapolated temperature values corresponding to different grid points as thermal boundary conditions, the temperature distributions were modelled in transient mode for different times. A typical plot for a 3 mm thick alumina sample is shown in Fig. 5 for the 10 s case. The material parameters, e.g. density (3900 kg/cm^3), Poisson's ratio (0.25), coefficient of thermal expansion (8.0×10^{-6}/°C), modulus of elasticity (350 GPa), thermal conductivity (8 W/m°C), heat capacity (1200 J/kg°C), etc., were introduced in the software for modelling studies.

The material properties were taken at room temperature values as the maximum temperature of the failure was between 340 and 700 °C which is in the short range compared to melting point of alumina. Moreover, for comparative studies such as effect of thickness on critical temperature difference, it is important to use the identical material properties for comparison.

3.1.4. Identification of maximum stressed zone

As per the modelling studies, the thermal stress was found to be maximum near the periphery of the top surface followed by the centre of the bottom surface. To verify the above observation, actual experiments were conducted with samples pre-indented at the expected maximum stressed locations, e.g. near the periphery of top surface and at the centre of the bottom surface (Fig. 6). Since, the induced cracks are bigger in size compared to in-situ flaws, the failure should initiate through the indent located at the maximum stressed zone. With this notion, three sets of indents were prepared on alumina samples by pre-cracking (i) near the periphery of the top surface (ii) at the centre of the bottom surface and (iii) at both periphery of top surface and centre of the bottom surface. Three samples were pre-cracked in each set with a load of 5 kg to generate flaws of 150–175 μm. The load 5 kg was chosen so that the flaw size should be well below the critical flaw size which is definitely quite more than because the sample did not crack when a flaw of this range was created by indentation with a 20 kg load. Since the samples are dense and well sintered, therefore, the inherent flaw size is expected to be very small.

The thermal shock tests were carried out as per the procedure discussed above. It was observed that the

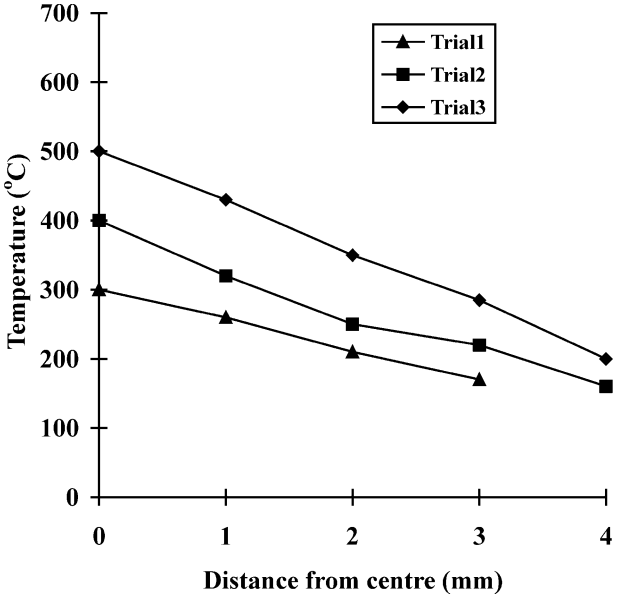

Fig. 3. Temperature distribution measured in an alumina disc (5 mm thick) during thermal shock test.

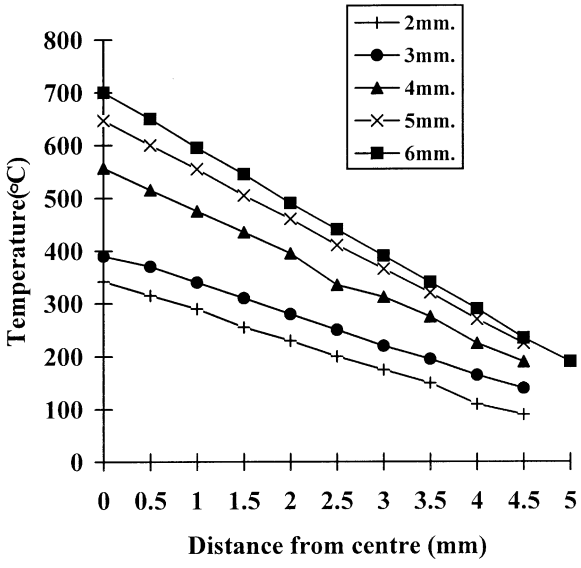

Fig. 4. Extrapolated temperatures for alumina of different thickness.

cracks passed through all the indents except for one sample having indents both at centre and at the periphery. In this case, the crack passed through the periphery but not at the centre. From the above set of experiments, it could be concluded that the cracks originated from the periphery of the top surface because, if, it would have originated from bottom centre, it need not have necessarily propagated in the direction of the

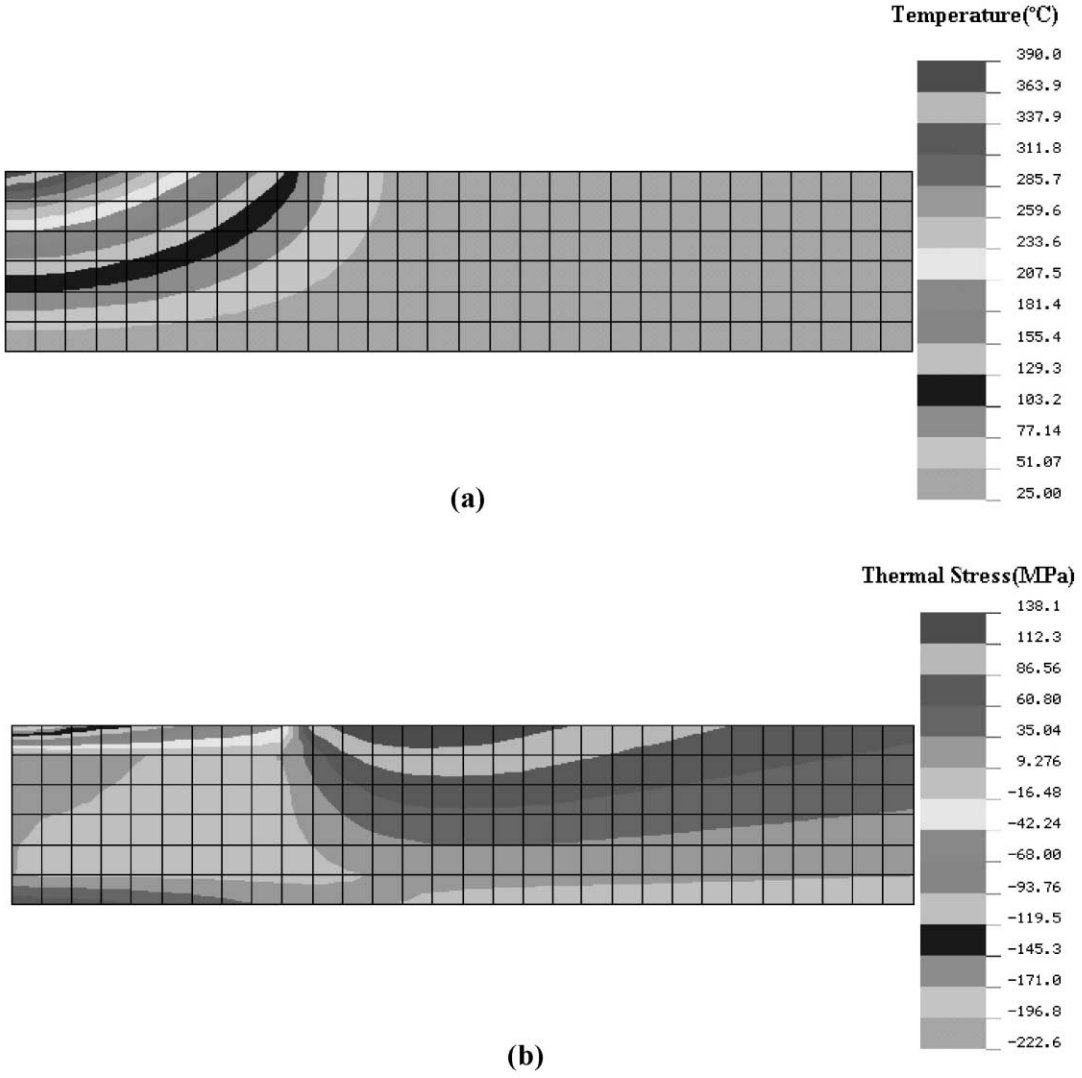

Fig. 5. (a) Temperature and (b) thermal stress profile generated in an alumina disc of 3 mm thickness by FEM.

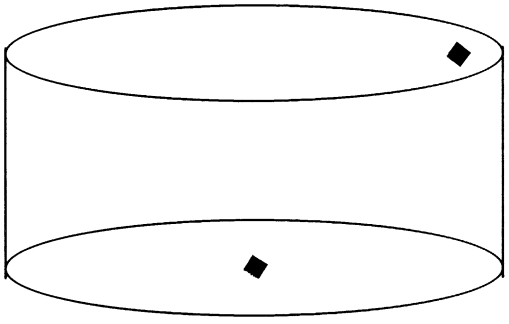

Fig. 6. Drawing of a typical alumina sample with an indent near the periphery of the top surface and an indent at the centre of bottom surface.

Table 3
The maximum thermal stress (tensile) resulted from the modelling of samples of different thickness

Sample thickness (mm)	Hot temperature (°C)	Thermal stress (MPa)
2	342	125.9
3	390	138.1
4	557	178.1
5	647	197.0
6	700	198.0

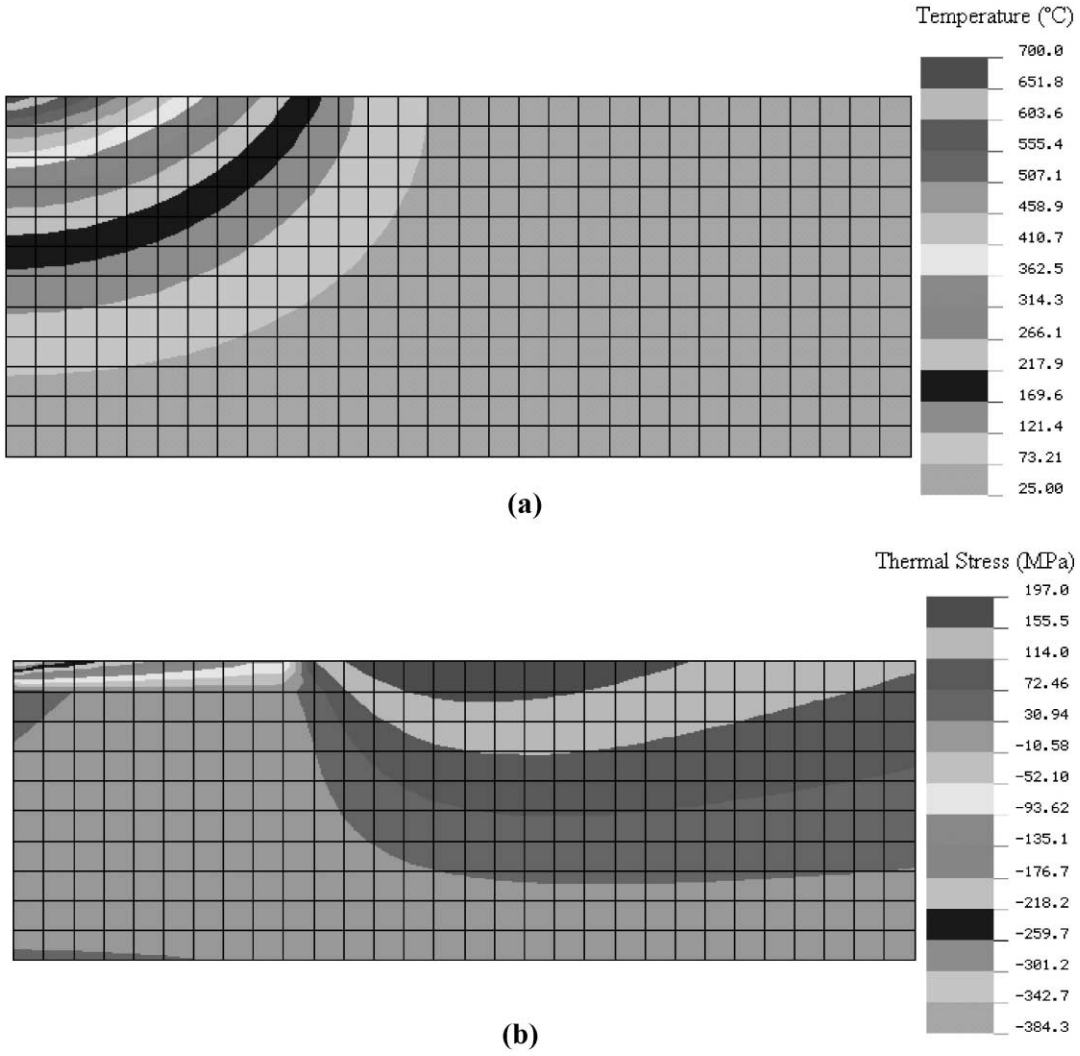

Fig. 7. (a) Temperature and (b) thermal stress profile generated in an alumina disc of 6 mm thickness by FEM.

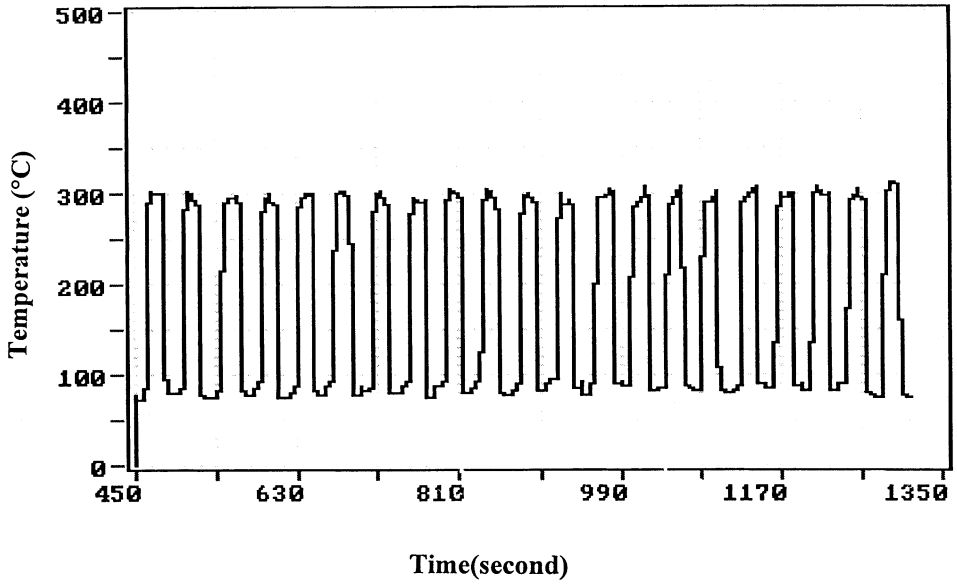

Fig. 8. Typical temperature cycles employed for thermal fatigue test of alumina.

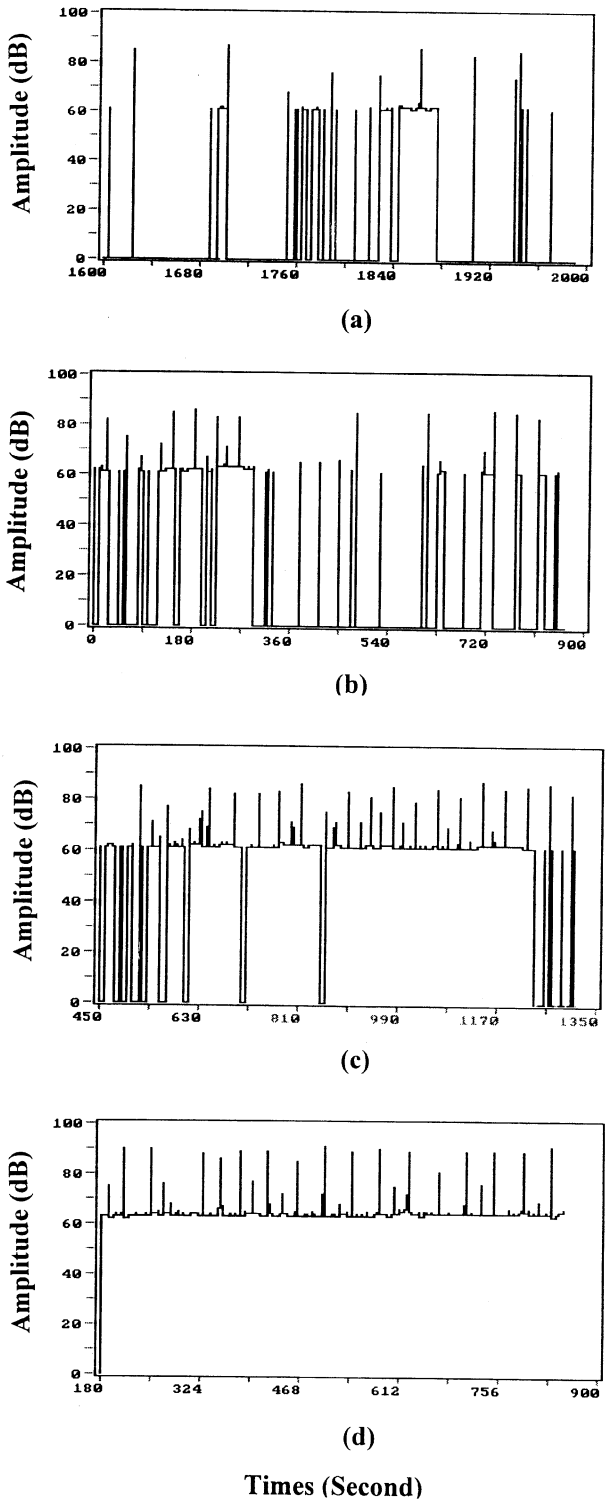

Fig. 9. Typical AE data generated during thermal fatigue cycles of alumina after (a) 50 (b) 100 (c) 150 and (d) 200 cycles of heating and cooling.

peripherally indented region. The results of modelling also supported the above assumption that the cracks originated from the periphery of the top surface of the sample where the stress was maximum.

3.1.5. Results of modelisation of thermal shock experimental studies

The thermal stress (tensile) values resulted from modelling of alumina samples of different thickness are presented below in Table 3.

From Table 3, It could be seen that a higher temperature is required to develop the same stress level for a thicker sample compared to a lower temperature required for a thinner sample. For example, a temperature of 390 °C is required to develop a stress of 138 MPa in the case of the 3 mm thick sample, while a temperature of 647 °C is required to develop a stress of 197 MPa in the case of 5 mm thick and about 700 °C is required developing the same stress in a 6 mm thick sample. Since the material fails after reaching the critical stress limit, thinner samples fail at lower temperatures as compared to thicker samples which is just opposite to quench experiments. A typical temperature and thermal stress distribution generated for a 6 mm alumina sample in a transient mode is presented in Fig. 7 in which the stress profile is presented in the form of bands to identify broadly the maximum stressed region from which a crack can originate probly from any point.

3.2. Thermal fatigue study of Al_2O_3

The thermal fatigue study of alumina samples of 5 mm thick was conducted with a maximum temperature in the range of 300–400 °C. The heating time and cooling time of each cycle were 15 and 20 s, respectively. The heating time was choosen to make sure the temperature stabilises at the maximum temperature and the cooling time was choosen based on the fact that before the start of a new fatigue cycle, the temperature of the sample should be same as that of the previous cycle, i.e. at room temperature. It was observed by the temperature measured by the thermocouple, accordingly, 20 s was chosen for identical quenching conditions. Due to high thermal mass of the copper block compared to the test sample and due to application of conducting paste at the interface and water circulation, the quenching temperature was brought down to room temperature very fast between the fatigue cycles.

It was observed that the sample did not crack even after 226 fatigue cycles with 400 °C as the maximum temperature which was very close to the critical temperature. However, lot of acoustic emission signals were registered as the number of cycles increased corresponding to formation of micro-cracks. The sample was investigated in an electron microscope which confirmed the presence of large number of small cracks similar to pitting corrosion. The sample did not fail after large number of fatigue cycles due to absence of a large crack growing up to critical size for failure. The presence of large number of small cracks also resulted in toughening by absorbing the heat energy by these cracks without

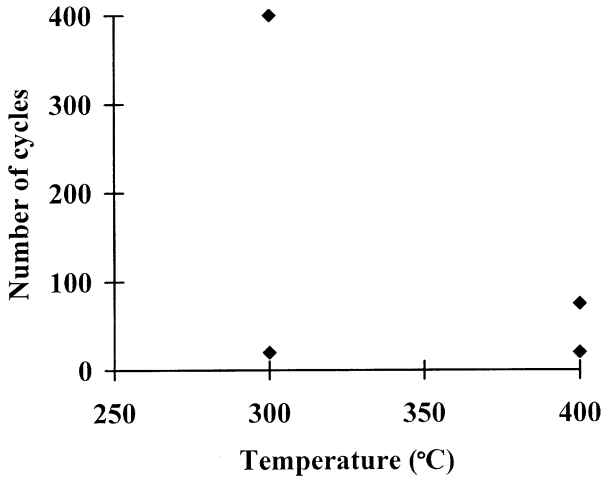

Fig. 10. Number of fatigue cycles vs. maximum temperature of cycles for samples with initial crack length of 2.5 kg (130 μm).

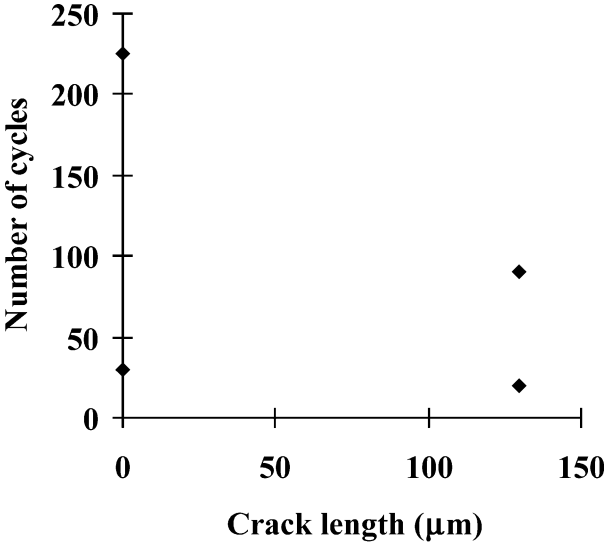

Fig. 11. Number of fatigue cycles (at 400 °C) vs. initial crack lengths.

allowing growing a single crack to failure. This phenomena is similar to that observed in zirconia system. A typical thermal fatigue test cycle with a maximum temperature of 300C and the acoustic emissions resulted are presented in Figs. 8 and 9, respectively. After 50 cycles, the AE resulted intermittently and around 200 cycles the AE was continuous (amplitude value being continuously at or above 60 dB) due to the generation of micro-cracks. Therefore, it was decided to pre-crack the specimens by indentation near the periphery (2 mm inside) so that the artificial cracks generated would propagate till failure.

3.2.1. Thermal fatigue test of pre-cracked specimens

Thermal fatigue tests were conducted by indenting near periphery of the heating surface so that it would experience maximum thermal stress during heating. The samples were indented with different loads ranging from 2.5 to 20 kg load. The indented samples were annealed at 600 °C for 4 h. The thermal fatigue tests were conducted at two different maximum temperatures (300 and 400 °C) with the same initial crack lengths and the results are presented in Fig. 10. Similarly, the results of thermal fatigue tests conducted at the maximum temperature of 400 °C with different initial crack lengths are presented in Fig. 11. From the figures, it could be seen that the number of fatigue cycles decreased sharply even at a minimum indentation load of 2.5 kg (crack length = 130 μm) compared to that without indentation. Similarly, the number of fatigue cycles decreased sharply by increasing the critical temperature by 100 °C for the samples indented with 2.5 kg load. The number of cycles was further reduced by high value of indentation load (20 kg). The acoustic emissions collected in the course of failure had interesting features.

3.3. Critical comments on the test results obtained

The preliminary results on thermal shock experiments confirm the effect of thickness on ΔT_C. ΔT_C or T_{max} is more for thicker samples unlike in the case of quench experiments in which higher ΔT_C is observed for thinner samples. However, thermal fatigue results and indentation experiments have shown similar trends as quench tests.

4. Conclusions

1. The thermal stress is maximum at periphery of the top surface, hence, the failure initiates from this region.
2. The critical temperature difference, ΔT_C was dependent on the thickness of the sample and was higher for thicker sample. This result is opposite to water quench method. This is because a higher temperature is necessary to develop the same stress level in a thicker sample. This was also confirmed by the modelling.
3. The critical temperature difference, ΔT_C, decreased with increase in the initial crack length similar to water quench method.
4. The number of thermal fatigue cycles decreased with increase in temperature difference of the cycles.
5. More experiments are in progress to refine the use of this novel and simple test set up to test various ceramic material to get more precise and reliable data.

Acknowledgements

The authors thank Mr. A. Cheluvaraju and Mr. V.A. Jaleel for their help rendered during the course of this study. The authors also thank Dr. C. Divakar and Mr.

Jayaprakash for their help during indentation studies. The authors are grateful to Indo-French Center for Promotion of Advanced Research, New Delhi, for the grant of a project (IFCPAR 1208–2) which made this study possible.

References

1. Lewis, D. Thermal shock and thermal shock fatigue testing of ceramics with the water quench test. In *Fracture Mechanics of Ceramics 6*, ed. R. C. Bradt, A. G. Evans, D. P. H. Hasselman and F. F. Lange. Plenum Press, New York, 1981, pp. 487–496.
2. Wei, G. C. and Walsh, J., Hot-gas-jet method and apparatus for thermal-shock testing. *J. Am. Ceram. Soc.*, 1989, **72**, 1286–1289.
3. Faber, K. T. and Evan, A. G., Quantitative studies of thermal shock resistance of ceramics based on a novel test technique. *J. Am. Ceram. Soc.*, 1981, **64**, 296–301.
4. Rogers, W. P. and Emery, A. F., Contact thermal shock tests of ceramics. *J. Mater. Sci.*, 1992, **27**, 46–152.
5. Anderson, T. and Rowcliffe, D. J., Indentation thermal shock test for ceramics. *J. Am. Ceram. Soc.*, 1996, **79**, 1509–1514.
6. Kamiya, N. and Kamigaito, O., Prediction of thermal fatigue life of ceramics. *J. Mat. Sci.*, 1979, **14**, 573–582.
7. Panda, P. K., Etude de l'Endommagement de Materiaux ceramiques par Choc thermique ascendant: Comportment a la Fatigue thermique et Modelisation. PhD thesis, INSA de Lyon, France, June 1999.
8. Mignard, M. F., Olagnan, C., Saadaoui, M. and Fantozi, G., Thermal shock behaviour of a coarse grain porous alumina. Part 1—temperature field determination. *J. Mat. Sci.*, 1996, **31**, 2131–2138.
9. Mignard, F., Olagnan, C., Saadaoui, M. and Fantozi, G., Thermal shock behaviour of a coarse grain porous Alumina. Part II—stress intensity factor and damage evaluation. *J. Mat. Sci.*, 1996, **31**, 2437–2441.
10. Gupta, T. K., Critical grain size for non catastrophic failure in Al_2O_3 subjected to thermal shock. *J. Am. Ceram. Soc.*, 1973, **6**, 281–298.
11. Panda, P. K., Kannan, T. S., Dubois, J., Olagnon, C. and Fantozzi, G., Thermal shock and thermal fatigue study of ceramic materials on a newly developed ascending thermal shock test equipment. *Science and Technology of Advanced Materials*. Submitted for publication.